

# Photoionization of the valence shells of the neutral tungsten atom

C P Ballance<sup>1</sup> and B M McLaughlin<sup>2,3†</sup>

<sup>1</sup>Department of Physics, 206 Allison Laboratory, Auburn University, Auburn, AL 36849, USA

<sup>2</sup>Centre for Theoretical Atomic, Molecular and Optical Physics (CTAMOP), School of Mathematics and Physics, The David Bates Building, 7 College Park, Queen's University Belfast, Belfast BT7 1NN, UK

<sup>3</sup>Institute for Theoretical Atomic and Molecular Physics, Harvard Smithsonian Center for Astrophysics, MS-14, Cambridge, MA 02138, USA

**Abstract.** Results from large-scale theoretical cross section calculations for the total photoionization of the 4f, 5s, 5p and 6s orbitals of the neutral tungsten atom using the Dirac Coulomb R-matrix approximation (DARC: Dirac-Atomic R-matrix codes) are presented. Comparisons are made with previous theoretical methods and prior experimental measurements. In previous experiments a time-resolved dual laser approach was employed for the photo-absorption of metal vapours and photo-absorption measurements on tungsten in a solid, using synchrotron radiation.

The lowest ground state level of neutral tungsten is  $5p^65d^46s^2\ ^5D_J$ , with  $J=0$ , and requires only a single dipole matrix for photoionization. To make a meaningful comparison with existing experimental measurements, we statistically average the large-scale theoretical PI cross sections from the levels associated with the ground state  $5p^65d^46s^2\ ^5D_J$  [ $J = 0, 1, 2, 3, 4$ ] levels and the  $5d^56s\ ^7S_3$  excited metastable level. As the experiments have a self-evident metastable component in their ground state measurement, averaging over the initial levels allows for a more consistent and realistic comparison to be made.

In the wider context, the absence of many detailed electron-impact excitation (EIE) experiments for tungsten and its multi-charged ion stages allows current photoionization measurements and theory to provide a road-map for future electron-impact excitation, ionization and di-electronic cross section calculations by identifying the dominant resonance structure and features across an energy range of hundreds of eV.

PACS numbers: 32.80.Fb, 31.15.Ar, 32.80.Hd, and 32.70.-n

Short title: Valence shell photoionization of neutral Tungsten

Submitted to: *J. Phys. B: At. Mol. Opt. Phys.* : 26 February 2015

† Corresponding authors, E-mail: ballance@physics.auburn.edu, b.mclaughlin@qub.ac.uk

## 1. Introduction

Material choice for the plasma facing components in fusion experiments is determined by competing desirables: on the one hand the material should have a high thermal conductivity, high threshold for melting and sputtering, low erosion rate under plasma contact, and on the other hand as a plasma impurity it should not cause excessive radiative energy loss.

For the ITER tokamak, currently under construction at Cadarache, France, Tungsten (symbol W, atomic number 74) is the favoured material for the wall regions of highest particle and heat load in a fusion reactor vessel, with beryllium for regions of lower heat and particle load. ITER is to start operation with a W-Be or W wall for the main D-D and D-T experimental programme. In support of ITER and looking ahead to the prospect of a fusion reactor other experimental plasma groups are also considering tungsten, including the ASDEX-Upgrade tokamak which now operates with an all-W wall and at JET, where a full ITER-like mixed W-Be-C wall is being installed. Smaller-scale experiments involving tungsten tiles are carried out on other tokamaks. The aforementioned attractive properties of tungsten mentioned above must be weighed against the negative fact that 74 ion stages have a great capacity to radiate power away. The consequence is that the burn condition for tungsten is not achievable for concentrations above  $2 \times 10^{-4}$ , and therefore theoretical models to accurately characterize impurity influx are required [1].

Atomic processes are central to energy transfer in magnetically confined plasmas. The energy balance in fusion devices such as tokamaks depends critically on how the plasma interacts with the walls of the vessel, therefore demanding accurate cross sections and associated rates for a wide variety of collisional processes.

These rates will enable us to understand and mitigate the causes of critical radiation losses that in minuscule concentrations prevent ignition. For modelling the behaviour of tungsten in a plasma a comprehensive understanding of various collisional processes is required for many ion stages. Beyond the first few charge states, open 4d and 4f shell configurations require complicated atomic structure calculations, and equally demanding electron-impact collisional calculations [2]. In the work of Ballance and co-workers [2], on electron-impact excitation, over 10,000 close-coupling channels were included in the theoretical model, however in the current photoionization studies we are only approaching the 5000 channel mark.

In contrast to electron-impact excitation/ionization calculations, photoionisation cross sections require only a few partial waves, governed by the dipole selection rules as compared to typically 50-60 partial waves required by electron-impact collisions. Furthermore, combined with currently available high resolution experiments for certain ion stages of W, theoretical DARC photoionization cross section calculations provide an ideal way to survey the first few ion stages of tungsten, indicating how well resonance structure is reproduced with a minimal atomic 9-12 configurations. This has future implications for the more intensive calculation of electron-ion recombination and ionization processes. In subsequent papers for the  $W^+ - W^{5+}$  ion stages, we intend to compare with more recent higher resolution experimental measurements already carried out at the Advanced Light Source, in Berkeley. However, for the single photoionization of neutral tungsten, only early experiments from the mid 1990s (which are not absolute) are available for comparison purposes. These early experiments employed a time-resolved dual-laser plasma technique to measure the photo-absorption of tungsten metal vapours [3]. These vapours were created by the

ablation of a spectroscopically pure tungsten solid, subject to a flashlamp pumped dye laser. A more complete description of the experiment is given in Costello *et al* [3, 4]. Photo-absorption experiments of W in a solid, as well as other neighbouring elements in the periodic table (Ta,Re) were measured in the photon energy range 30-600 eV using synchrotron radiation [5], at the 7.5-GeV electron synchrotron facility DESY. Sladeczek *et al* [6] prepared the tungsten target by the thermal evaporation from the metal at a temperature of 3200 K, to measure the photo-ion yield spectra of  $W^+$  in the energy region of 30-60 eV.

In the current investigation we also show a theoretical comparison, for photoionization (PI) cross sections between the present results obtained from a Dirac Coulomb R-matrix approximation (DARC) with the earlier Many-Bodied Perturbation Theory (MBPT) work of Boyle and co-workers [7].

The remainder of this paper is structured as follows. Section 2 presents a brief outline of the theoretical work. Section 3 presents a discussion of the results obtained from both the experimental and theoretical methods. Finally in section 4 conclusions are drawn from the present investigation.

## 2. Theory

An efficient parallel version [8] of the DARC [9, 10, 11, 12] suite of codes has been developed [13, 14, 15] to address the challenge of electron and photon interactions with atomic systems catering for several thousands of scattering channels. Metastable states are populated in these experiments and therefore additional theoretical calculations are carried out to gauge their extent. Recent modifications to the Dirac-Atomic-R-matrix-Codes, as implemented for (DARC) [13, 15, 14] allowed high quality photoionization cross section calculations of Fe-peak elements and Mid-Z atoms of interest to astrophysics. Cross-section calculations for trans-Fe element single photoionization of  $Se^+$ ,  $Xe^+$ ,  $Xe^{7+}$ ,  $Kr^+$  ions [14, 15, 16, 17],  $Si^+$  ions [18], and neutral Sulfur [19] have been made using the DARC code and have shown suitable agreement with high resolution measurements made at third generation light sources. In particular for the calculations presented here, the capacity to assign an arbitrary number of processors to the concurrent formation of every dipole matrix, mitigates the fact that matrix multiplications of eigenvector matrices over 60,000 by 60,000 in size require at least  $2 \times 10^{14}$  operations each.

All the present photoionization cross section calculations were performed in the Dirac Coulomb R-matrix approximation using our recently developed parallel version of the DARC codes [14, 15, 20]. The current state-of-the-art parallel DARC codes running on high performance computers (HPC) world-wide, allows one to concurrently form and diagonalize large-scale Hamiltonian and dipole matrices [21, 22] required for electron or photon collisions with atomic systems. This enables large-scale cross-section calculations to be completed in a timely manner.

### 2.1. Tungsten (W)

Photoionization cross sections on this complex system were performed for the ground and the excited metastable levels associated with the  $5s^25p^65d^46s^2 : ^5D$  term, and benchmarked with several available experimental measurements. We note that for neutral and or near neutral heavy atoms determining their atomic structure sufficiently

**Table 1.** Comparison of the theoretical energies using the GRASP code with the NIST [26] tabulated data; relative energies are in Rydbergs. A sample of the 17 lowest NIST levels of the residual  $W^+$  ion compared with our theoretical values from the 645-level approximation are presented .

Level	Configuration	Term	NIST Energy (Ryd)	GRASP Energy <sup>a</sup> (Ryd)	$\Delta^\dagger$ 645 levels
1	$5d^4(^5D)6s$	$^6D_{1/2}$	0.000000	0.000000	0.0
2	$5d^4(^5D)6s$	$^6D_{3/2}$	0.013841	0.009202	0.0046
3	$5d^4(^5D)6s$	$^6D_{5/2}$	0.028910	0.021266	0.0076
4	$5d^4(^5D)6s$	$^6D_{7/2}$	0.042978	0.034552	0.0084
5	$5d^4(^5D)6s$	$^6D_{9/2}$	0.056016	0.048546	0.0075
6	$5d^5$	$^6S_{5/2}$	0.067618	0.075682	0.0081
7	$5d^36s^2$	$^4F_{3/2}$	0.079383	0.119217	0.0398
8	$5d^36s^2$	$^4F_{1/2}$	0.080490	0.105601	0.0252
9	$5d^36s^2$	$^4F_{3/2}$	0.096526	0.133134	0.0366
10	$5d^36s^2$	$^4F_{5/2}$	0.102983	0.142539	0.0396
11	$5d^36s^2$	$^4F_{7/2}$	0.122219	0.157617	0.0354
12	$5d^4(^5D)6s$	$^4D_{1/2}$	0.120044	0.159874	0.0398
13	$5d^4(^5D)6s$	$^4D_{5/2}$	0.122242	0.150617	0.0284
14	$5d^4(^5D)6s$	$^4D_{3/2}$	0.133358	0.171186	0.0378
15	$5d^4(^5D)6s$	$^4D_{7/2}$	–	0.173779	–
16	$5d^4(^5D)6s$	$^4D_{9/2}$	0.135388	0.166293	0.0309
17	$5d^4(^5D)6s$	$^4D_{5/2}$	0.136396	0.177468	0.0411

<sup>a</sup> Theoretical energies from the 645-level approximation

<sup>†</sup> $\Delta$  Absolute difference in Rydbergs relative to NIST tabulations [26].

accurately is notoriously difficult. The atomic structure calculations optimized on the residual  $W^+$  ion were carried out using the GRASP code [23, 24, 25].

Our first close-coupling calculation employed the lowest 645 energy accessible levels arising from the nine configurations of the  $W^+$  residual ion:  $4p^64d^{10}4f^{14}5s^25p^65d^46s$ ,  $4p^64d^{10}4f^{14}5s^25p^65d^36s^2$ ,  $4p^64d^{10}4f^{14}5s^25p^55d^46s^2$ ,  $4p^64d^{10}4f^{14}5s^25p^65d^46s^2$ , we also opened the 4f-shell, namely,  $4p^64d^{10}4f^{13}5s^25p^65d^46s^2$ ,  $4p^64d^{10}4f^{13}5s^25p^65d^56s$ , then the 4d-shell,  $4p^64d^94f^{14}5s^25p^65d^46s^2$ , the 4p-shell,  $4p^54d^{10}4f^{14}5s^25p^65d^46s^2$  and finally the 4s-shell,  $4s4p^64d^{10}4f^{14}5s^25p^65d^46s^2$ .

In Table 1, we compare a representative sample of our energy levels with the NIST tabulated values [26] for the residual ion  $W^+$ . We find that the maximum energy difference is typically of the order of 0.04 Rydbergs for the valence  $n = 5$  and  $n = 6$  shell levels, with no available energies given for the open  $n = 4$  shell levels. This is well within the metastable uncertainty of the experimental measurements. In the second calculation, we included all possible 1227 levels from the last 9 configurations in order to complete the total photoionization of the remaining  $n = 4$  shell up to a photon energy of 600 eV. The 4d direct ionization begins at 257.5 eV, the 4p direct ionization at approximately 442 eV and the 4s direct ionization at 616 eV.

Photoionization cross section calculations for a 645-level and a 1227-level model were performed in the Dirac-Coulomb approximation using the DARC codes [14, 15, 21, 22] for the ground and metastable fine-structure levels associated with the  $5s^25p^65d^46s^2$  configuration

**Table 2.** Number of Scattering Channels associated with each dipole allowed symmetry

Even Symmetry	Number of Channels	Odd Symmetry	Number of Channels
$J = 0$	645	$J' = 0$	645
$J = 1$	1872	$J' = 1$	1872
$J = 2$	2929	$J' = 2$	2929
$J = 3$	3750	$J' = 3$	3750
$J = 4$	4320	$J' = 4$	4320
$J = 5$	-	$J' = 5$	4671

The R-matrix boundary radius of 12 Bohr radii was sufficient to envelop the radial extent of the residual  $W^+$  ion atomic orbitals. A basis of 16 continuum orbitals was sufficient to span the incident experimental photon energy range from threshold up to 120 eV for the 645-level model and 30 continuum basis orbitals to span 0-625 eV for the 1227 model. Since dipole selection rules apply, total ground-state photoionization cross sections require only the  $J^\pi = 0^e \rightarrow J'\pi' = 1^o$ , bound-free dipole matrix. In the case of the excited metastable states the  $J^\pi = 4^e \rightarrow J'\pi' = 5^o, 4^o, 3^o$ ,  $J^\pi = 3^e \rightarrow J'\pi' = 4^o, 3^o, 2^o$ ,  $J^\pi = 2^e \rightarrow J'\pi' = 3^o, 2^o, 1^o$  and  $J^\pi = 1^e \rightarrow J'\pi' = 2^o, 1^o, 0^o$  are necessary.

We note that the present investigations are currently the largest photoionization calculations in terms of the number of scattering channel performed to date with our DARC codes. For example, in the case of the initial  $J = 4$  metastable level, we have a  $J = 5^o$  symmetry with 4,761 scattering channels and matrices of the size of 60,723 to consider in the photoionization calculation. In table 2, we list the number of channels associated with each of the  $J - J'$  dipole pairs used in the statistically averaged comparison with experiment, also allowing for the fact that the  $5d^56s$ ,  $J = 3$  excited level lies energetically below the  $5d^46s^4$ ,  $J = 3$  of the neutral tungsten ground state configuration.

## 2.2. Photoionization cross sections

For the ground and metastable initial states of the neutral W atom studied here, the outer region collision problem was solved (in the resonance region below and between all thresholds) using a suitably chosen fine energy mesh of  $6.0 \times 10^{-4}$  Rydbergs ( $\approx 8.0$  meV), in order to resolve all important resonance structure in the appropriate photoionization cross sections. This is sufficient for comparison purposes with the previous experimental results [5, 3, 6] which were taken at resolutions ranging from 0.25 eV (250 meV) to 0.5 eV (500 meV).

To simulate the experimental measurements, the DARC theoretical photoionization cross section results have been convoluted with a Gaussian having a profile of full width half maximum (FWHM) similar to the experimental resolution. In order to compare with experiment, we have statistically weighted the ground and metastable photoionization cross sections as well as the initial bound level. This has the effect of reducing the actual photoionization threshold, due to the excited states of the  $^5D$  having consistently higher quantum numbers. Comparatively, it also reduces the absolute heights of the resonance structure between 40 and 60 eV as opposed to the  $J = 0 - 1$

calculation, but otherwise the individual 5 level-resolved cross sections are remarkably similar.

We note that there are other metastable levels from the same initial  $5d^46s^2$  configuration up to at least 0.285 Rydbergs above the ground state, leading to energy differences of up to 3 eV when comparing the energy scale with experimental measurements. A complete direct modelling comparison with experiment would require the calculation of photoionization cross sections from all the 34 levels of the ground state configuration, and probably approximately 50 levels from the  $5d^56s$  and  $5d^46s6p$  configurations that are interspersed among them. However, as we only have access to finite computational resources these extra 79 calculations in addition to the 5 presented here are beyond present capabilities.

### 3. Results and Discussion

The calculated ionization potential from our DARC calculation is 8.09 eV which is 230 meV above the NIST tabulated value of 7.86 eV. However the statistically averaged initial bound state reduces this difference to a value of 170 meV, bringing it closer to the experimental value.

As Fig.1 illustrates, collectively the direct photoionization of the 6s and 5d orbitals peak at 30 Mb at a photon energy of 19 eV. However, it is the direct photoionization of the 4f and the 5p orbitals, and the associated 4f – 5d and 5p – 5d resonances that dominate the cross section from 40-65 eV, with narrow peaks as high as 75-80 Mb. The 5s photoionization is evident from 65 eV onwards, but only marginally so. The onset of our 4f photoionization at approximately 38-39 eV slightly leads the 5p photoionization by 1-2 eV, and it agrees well with the MBPT theory in terms of energy position. However the MBPT theoretical cross sections are persistently lower across the entire energy range. Between 43 eV and 54 eV, our model has several hundred thresholds belonging to either  $4p^64d^{10}4f^{13}5s^25p^65d^46s^2$  or  $4p^64d^{10}4f^{14}5s^25p^55d^46s^2$  configurations thus making it difficult to determine the relative strength of each. The sharp resonance at 35 eV, identified in the Sladeczek experiment [6] which they attributed to a 5p – 6s transition, is well reproduced by the current DARC model.

In Fig.2, we compare the ground state term statistically averaged PI cross section results with the experiments of Costello *et al* [3] and those of Haensel *et al* [5]. At 35 eV, the dual laser experiment exhibits the onset of the 4f ionization at approximately 3 - 4 eV, before both the theoretical values of the MBPT [7] and the present DARC PI cross section calculations, however still within the range of the other higher levels of the  $6s^2$  configuration as reported in the NIST energy level table. This suggests that the metastable component of the experiment of Costello and co-workers [3] may include some of these higher levels. The Haensel experiment [5], from a solid-state target does not exhibit the strong 4f-5d, or 5p-5d resonance structure to the same extent compared to all presented theories and the dual-laser experiment. The Sladeczek experiment [6] (also from a solid perspective), does not provide absolute values either, but in terms of a relative minimum to maximum ratio of the measurement is comparable to the Haensel and co-workers [5] experimental result. Sladeczek and co-workers [6] do however report a relativistic Hartree-Fock calculation which is a mixture of the first six levels of neutral tungsten. We have employed these same six mixing coefficients with our present DARC PI cross section results, represented by the dashed-line in Fig.2. Not surprisingly, as the individual PI cross sections are remarkably similar, (shifted slightly only by energy differences in the target), it provides a result very close to the

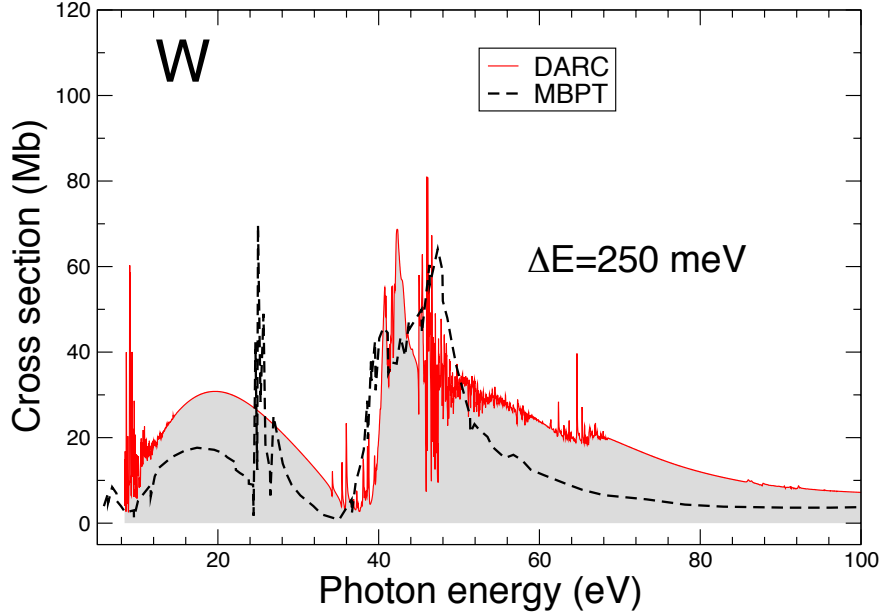


**Figure 1.** (Colour online) Single photoionization of neutral W over the photon energy range 8 eV - 100 eV. The solid line and corresponding shaded area correspond to the total photoionization of the 6s, 5p, 5s and 4f orbitals from the  $J = 0 : 6s^2$  tungsten ground state. Cross sections are given in Mb. The present DARC calculations were Gaussian convolved at FWHM 250 meV. The dashed line corresponds to the earlier MBPT [7] calculation for the ground state level.

prediction of the statistically averaged DARC result.

Comparison with other theoretical methods is a much simpler prospect than with experimental measurement. There are no unwanted metastable components to contend with and it requires the calculation of a single  $J = 0 - J' = 1$  dipole matrix as is illustrated in Fig.1. The reduced number of associated channels with partial waves of low angular momentum has allowed us to increase the photon energy range up to 625 eV, as illustrated in Fig.3. Here we extend our DARC PI cross section calculations to span the energy to encompass the photoionization energy range of all the  $n=4, 5$  and 6 shells. Above 100 eV, the direct ionization of the 4d, 4p and 4s orbitals is minimal compared with the preceding sub-shells. The Rydberg resonances attached to the upper levels of each hole configuration are much more evident than the direct total photoionization above 200 eV. The photoionisation of the 4f orbital is the dominant component of the total photoionisation cross section in this energy range.

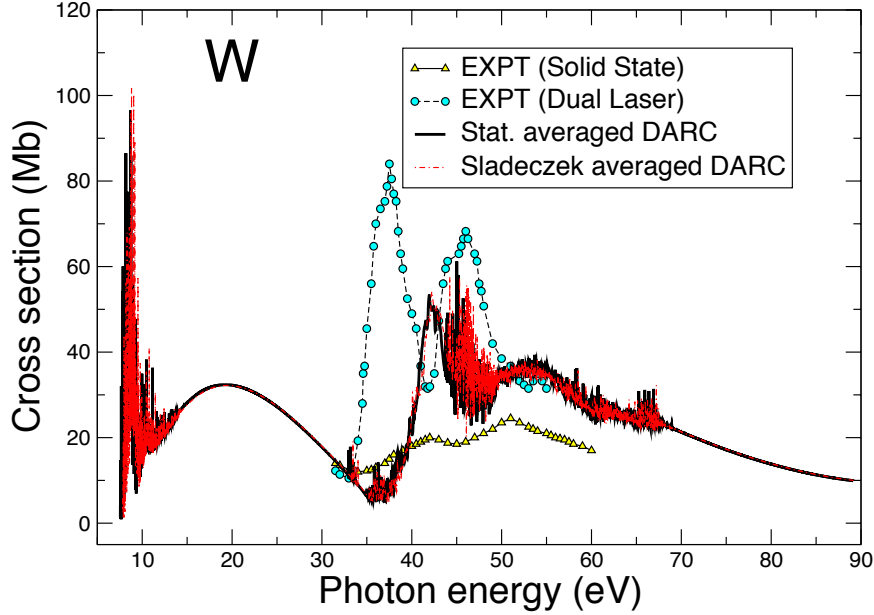


**Figure 2.** (Colour online) Single photoionization of neutral W over the photon energy range 8 eV - 100 eV, comparing weighted averaged theoretical calculations with several different experiments. The DARC results (645-levels approximation, solid black line), are the statistical average of the 5 levels associated the  $^5D$  term ground state. The (dashed red-line) is the weighted DARC results of the lowest 6 levels, employing the mixing coefficients reported by Sladeczek and co-workers [6]. Solid circles with dashed line are the dual-laser experimental results of Costello and co-workers [3] and the solid triangles are the results from the experimental work of Haensel and co-workers [5]. The statistically averaged DARC PI cross sections were Gaussian convolved at a FWHM of 250 meV.

#### 4. Conclusions

Photoionization cross sections calculations for the neutral tungsten atom were obtained from large-scale close-coupling calculations within the Dirac-Coulomb R-matrix approximation (DARC) and compared with moderately resolved experimental measurements.

The neutral tungsten photoionization presented here shall complement a future series of studies on tungsten ions  $W^{q+}$  in low charged states up to  $q = 5$  [27, 28, 20]. The comparison of the measured photoionization spectra with large-scale R-matrix close-coupling calculations presented here shows good agreement, and it is expected that applying a similar approach to other charged states of tungsten that have been investigated by more recent experiments at ALS will provide valuable interpretation of those measurements. It is hoped that the present theoretical work will act as a stimulus and encourage new experimental studies on neutral tungsten photoionization



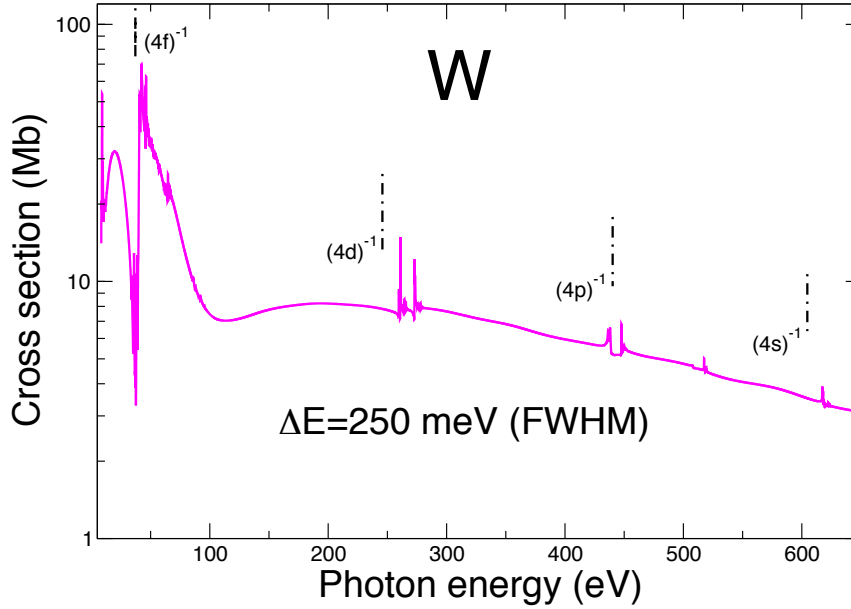


**Figure 3.** (Colour online) Single photoionization cross sections of neutral W over the photon energy range 8 eV - 625 eV, from the present DARC PI calculations incorporating 1227 levels in the close-coupling calculations. The photoionization threshold of each of the  $4\ell^{-1}$  orbitals hole configurations are indicated on the graph.

at the same high resolution achieved by the other ion stages of this system.

### Acknowledgments

C P Ballance was supported by NSF and NASA grants through Auburn University. B M McLaughlin acknowledges support by the US National Science Foundation through a grant to ITAMP at the Harvard-Smithsonian Center for Astrophysics, Queen's University Belfast for the award of a visiting research fellowship (VRF) and the hospitality of the University of Auburn during a research recent visit. The computational work was carried out at the National Energy Research Scientific Computing Center in Oakland, CA, USA and at the High Performance Computing Center Stuttgart (HLRS) of the University of Stuttgart, Stuttgart, Germany. This research also used resources of the Oak Ridge Leadership Computing Facility at the Oak Ridge National Laboratory, which is supported by the Office of Science of the U.S. Department of Energy under Contract No. DE-AC05-00OR22725. Helpful discussions with Professor E T Kennedy are gratefully acknowledged.

## References

- [1] ITER, URL <http://www.iter.org/>
- [2] Ballance C P, Loch S D, Pindzola M S and Griffin D C 2013 *J. Phys. B: At. Mol. Opt. Phys.* **46** 1
- [3] Costello J T, Kennedy E T, Sonntag B F and Cromer C L, 1991 *J. Phys. B* **B 24** 5063
- [4] Costello J T, Kennedy E T, Sonntag B F, Cromer C L and C W Clarke 1991 *Phys. Rev. A* **43** 1441
- [5] Haensel R, Radler K, Sonntag B and Kunz C, 1969 *Solid State Commun.* **7** 1495
- [6] Sladeczek P, Feist H, Feldt M, Martins M and Zimmerman P 1995 *Phys. Rev. Lett.* **70** 1483
- [7] Boyle J J, Altun Z and Kelly H P 1993 *Phys. Rev. A* **47** 4811
- [8] Ballance C P and Griffin D C 2006 *J. Phys. B: At. Mol. Opt. Phys.* **39** 3617
- [9] Norrington P H and Grant I P 1987 *J. Phys. B: At. Mol. Opt. Phys.* **20** 4869
- [10] Wijesundera W P, Parpia F A, Grant I P and Norrington P H 1991 *J. Phys. B: At. Mol. Opt. Phys.* **24** 1803
- [11] Norrington P H 1991 *J. Phys. B: At. Mol. Opt. Phys.* **24** 1803
- [12] DARC codes URL <http://web.am.qub.ac.uk/DARC>, <http://connorb.freeshell.org>
- [13] Fivet V, Bautista M A and Ballance C P 2012 *J. Phys. B: At. Mol. Opt. Phys.* **45** 035201
- [14] McLaughlin B M and Ballance C P 2012 *J. Phys. B: At. Mol. Opt. Phys.* **45** 095202
- [15] McLaughlin B M and Ballance C P 2012 *J. Phys. B: At. Mol. Opt. Phys.* **45** 085701
- [16] Müller A, Schipper S, Esteves-Macaluso D, Habbi M, Aguilar A, Kilcoyne A L D, Phaneuf R A, Ballance C P and McLaughlin B M 2014 *J. Phys. B: At. Mol. Opt. Phys.* **47** 215202
- [17] Hinojosa G, Covington A M, Alna'Washi G A, Lu M, Phaneuf R A, Sant'Anna M M, Cisneros C, Álvarez I, Aguilar A, Kilcoyne, Schlachter A S, Ballance C P and McLaughlin B M 2012 *Phys. Rev. A* **86** 063402
- [18] Kennedy E T, Mosnier J -P, Van Kampen P, Cubaynes D, Guilband S, Blancard C, McLaughlin B M and J M Bizau J M 2014 *Phys. Rev.* **90** 063409 URL <http://journals.aps.org/prabstract/10.1103/PhysRevA.90.063409>
- [19] Barthel M, Flesch R, Rühl E and McLaughlin B M 2015 *Phys. Rev. A* **91** 013406 URL <http://journals.aps.org/prabstract/10.1103/PhysRevA.91.013406>
- [20] Müller A M, Schippers S, Hellhund J, Kilcoyne A L D, Phaneuf R A, Ballance C P and McLaughlin B M 2014 *J. Phys. Conf. Ser.* **488** 022032
- [21] McLaughlin B M and Ballance C P 2014 Petascale computations for Large-scale Atomic and Molecular collisions *Sustained Simulated Performance 2014* Chapter 15 ed Resch M M, Kovalenko Y, Focht E, Bez W and Kobaysahi H (New York and Berlin: Springer)
- [22] McLaughlin B M, Ballance C P, Pindzola M S and Müller A 2014 PAMOP: Petascale Atomic, Molecular and Optical Collisions *High Performance Computing in Science and Engineering '14* Chapter 4 ed Nagel W E, Kröner D H and Resch M M (New York and Berlin: Springer)
- [23] Dyall K G, Grant I P, Johnson C T and Plummer E P 1989 *Comput. Phys. Commun.* **55** 425
- [24] Parpia F, Froese Fischer C and Grant I P 2006 *Comput. Phys. Commun.* **94** 249
- [25] Grant I P 2007 *Quantum Theory of Atoms and Molecules: Theory and Computation* (New York, USA: Springer)
- [26] Kramida A E, Ralchenko Y, Reader J, and NIST ASD Team, NIST Atomic Spectra Database (version 5), National Institute of Standards and Technology, Gaithersburg, MD, USA URL [http://physics.nist.gov/PhysRefData/ASD/levels\\_form.html](http://physics.nist.gov/PhysRefData/ASD/levels_form.html)
- [27] Müller A M, Schippers S, Kilcoyne A L D and Esteves D 2011 *Phys. Scr.* **T144** 014052
- [28] Müller A M, Schippers S, Kilcoyne A L D, Aguilar A, Esteves D and Phaneuf R A 2012 *J. Phys. Conf. Ser.* **388** 022037